

Efficient Increase of DNA Cleavage Activity of a Diiron(III) Complex by a Conjugating Acridine Group

Xiao-Qiang Chen,^[a] Xiao-Jun Peng,^{*[a]} Jing-Yun Wang,^[b] Yan Wang,^[b] Song Wu,^[b] Li-Zhu Zhang,^[a] Tong Wu,^[a] and Yun-Kou Wu^[a]

Keywords: DNA cleavage / Iron complex / Diiron(III) complex / Intercalator / Acridine

A new diferric complex, Fe₂L_b, in which a DNA intercalator (acridine) is linked to a precursor diferric complex (Fe₂L_a), has been designed and synthesised as a hydrolytic cleaving agent of DNA. Compared with Fe₂L_a (without the DNA intercalator) (L_a: 2,6-bis{[(2-hydroxybenzyl)(pyridin-2-yl)methylamino]methyl}-4-methylphenol), Fe₂L_b [L_b: 5-(acridin-9-yl)-N-(3,5-bis{[(2-hydroxybenzyl)(pyridin-2-yl)methylamino]methyl}-4-hydroxybenzyl)pentanamide] leads to a 14-fold increase in the cleavage efficiency of plasmid DNA due to the binding interaction between DNA and the acridine moiety. The interaction has been demonstrated by UV/Vis absorption, CD spectroscopy, viscosity experiments and thermal denaturation studies. The hydrolytic mechanism is supported by evidence from T4 DNA ligase assay, reactive oxygen spe-

cies (ROS) quenching and BNPP [bis(4-nitrophenyl) phosphate, a DNA model] cleavage experiments. The pH dependence of the BNPP cleavage by Fe₂L_a in aqueous buffer media shows a bell-shaped pH-*k*_{obs} profile with an optimum point around a pH of 7.0 which is in good agreement with the maximum point of the pH-dependent relative concentration curve of active species from the pH titration experiments. The determination of the initial rates at a pH of 7.36 as a function of substrate concentration reveals saturation kinetics with Michaelis–Menten-like behaviour and Fe₂L_a shows a rate acceleration increase of 4.7 × 10⁶ times in the hydrolysis of BNPP.

(© Wiley-VCH Verlag GmbH & Co. KGaA, 69451 Weinheim, Germany, 2007)

Introduction

Mimicking the activities of nucleases is currently an attractive research area in molecular biology and therapy owing to its essential role in artificial restriction enzyme and conformational probes of nucleic acids.^[1–4] A number of oxidative cleavage reagents have been used with great success in DNA footprinting^[5] for locating base mismatches and loop regions,^[6] for locating conformational variations in DNA^[7] and as chemotherapeutic agents.^[8] However, these oxidative cleavage agents require the addition of an external agent (e.g., light or hydrogen peroxide) to initiate cleavage. Furthermore, oxidative cleavage is mediated by reactive oxygen species (ROS) which can cause other severe cytotoxic effects. These drawbacks of the oxidative reagents hinder their potential applications in vivo. For eliminating the possibility of significant cytotoxic side effect of ROS, pathways that result in DNA cleavage by hydrolysis mechanisms have been considered to be preferable. However, the

phosphodiester bonds of DNA are exceptionally resistant to hydrolysis under physiological conditions and it is a great challenge to find new catalysts to enhance the hydrolysis.^[9–11] In the past decade, a variety of metal complexes which can promote the hydrolysis of DNA and phosphodiester esters have been reported, including complexes based on Cu^{II}, Zn^{II}, Co^{III} and lanthanide ions.^[12–21] Furthermore, many elegant dinuclear complexes have been developed as structural or functional models of the enzymes.^[22] Compared with mononuclear complexes, dinuclear complexes have the higher activity as a result of the cooperative interaction of metal ions in stabilising the transition state of phosphodiester cleavage.

Among the physiologically relevant metal ions, iron has been much less studied in the hydrolytic reaction^[23–25] due to the fact that Fe-dependent DNA cleavage is often involved in oxygen free radical processes such as the Fenton reaction. In fact, purple acid phosphatases (PAP), comprising diiron active centers can catalyse the hydrolysis of certain phosphate esters, including nucleoside di- and triphosphates and aryl phosphates under weakly acidic conditions.^[26] On the other hand, many efforts have so far been made to enhance the reactivity of metal complexes cleaving DNA. One of these strategies is the conjunction of metal complexes and intercalating groups to increase the DNA affinity of cleavage agents.^[27–29] Tecilla et al. synthesised a series of Zn^{II} complex-intercalator conjugates, the struc-

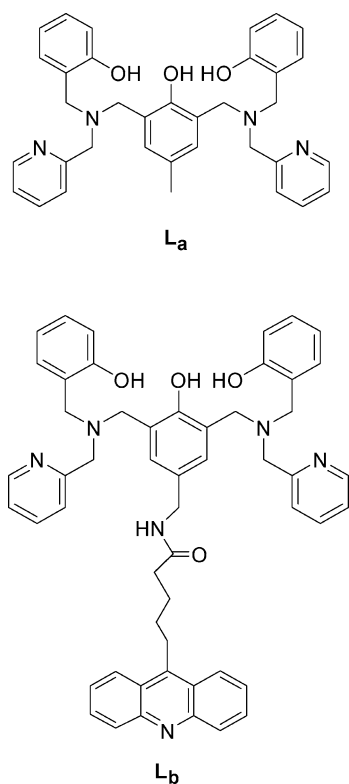
[a] State Key Laboratory of Fine Chemicals, Dalian University of Technology, 158 Zhongshan Road, Dalian 116012, P. R. China
Fax: +86-411-88993906
E-mail: pengxj@dut.edu.cn

[b] Department of Bioscience and Biotechnology, Dalian University of Technology, Dalian 116023, P. R. China

Supporting information for this article is available on the WWW under <http://www.eurjic.org> or from the author.

tures of which feature a *cis,cis*-triaminocyclohexane chelating subunit linked to an anthraquinone moiety through alkyl spacers with different lengths and reactivity studies showed that the length of the spacer which tethers the intercalating unit to the catalytic group is a key element in the cleavage activity.^[28] An earlier complex was reported by Lawrence and co-workers, who appended acridine to a pentadentate N5 ligand and used it as a cofactor for Fe^{II}-promoted DNA oxidative cleavage.^[29] However, examples of dinuclear complexes appended to the intercalating groups as hydrolytic agents are surprisingly rare.

In our work, the new diferric complex Fe₂L_b is derived from L_b (Scheme 1), the structure of which features a binuclear Fe^{III} complex subunit linked an acridine moiety through a long spacer. The intercalating role of acridine has been confirmed by UV/Vis absorption, CD spectroscopy, viscosity experiments and thermal denaturation studies. The hydrolytic role of the diiron(III) subunit has also been confirmed from the efficient cleavage of the BNPP [bis(4-nitrophenyl) phosphate]. Furthermore, the conjugate can effectively promote the hydrolysis of plasmid DNA.



Scheme 1. Molecular structures of ligands used.

Results and Discussion

Synthesis and Characterisation

L_a was prepared according to a procedure previously described by Neves et al.^[30] L_b was synthesised according to the reaction sequences depicted in Scheme S1. The previous report by Tecilla and co-workers has shown that the flexible

spacer is very important in enhancing the activity of the conjugate toward DNA cleavage. Consequently, 5-(acridin-9-yl)pentanoic acid was chosen to link with the dinuclear metal moiety through an imide bond.^[28] The acid was synthesised according to the method provided by Nadukkudy et al.^[31] The compound 2-[3,5-bis(chloromethyl)-4-hydroxybenzyl]isoindole-1,3-dione, reported in our earlier publications,^[32] was incubated with 2-[[pyridin-2-ylmethyl]amino]methylphenol in the presence of triethylamine to yield the intermediate **2**. After deprotection of **2** with hydrazine hydrate in ethanol at room temperature, the amine obtained was then linked to the acridinium subunit by an amide bond to afford the ligand L_b in a yield of 50%. The diiron(III) complex [Fe^{III}₂(BBPMP)(μ-OAc)₂] with acetate bridging groups using L_a as a ligand has been previously reported by Neves and co-workers.^[30] In accordance with this report, we initially obtained two complexes with acetate bridging groups using L_a and L_b. Unfortunately, the solubilities in water were too low to carry out DNA experiments. Based on the modified synthesis, the complexes Fe₂L_a and Fe₂L_b were obtained and both have high solubility in water. Attempts to obtain the structures of Fe₂L_a and Fe₂L_b by X-ray diffraction were not successful although Fe₂L_a and Fe₂L_b were characterised by elemental analysis and spectroscopic methods (see Figures S1–S11 in the electronic supporting information). The binuclear structures of the complexes were supported by the calculated isotopic distributions which are in agreement with those measured using high-resolution ESI-MS (Figures S2 and S6–S9, supporting information). For Fe₂L_a, the observed species at *m/z* (*z* = 1) = 731.1150 corresponds to the singly-charged diiron species [Fe^{III}₂(L_{a-3H})(OCH₃)₂]⁺. The six positive charges due to the two Fe³⁺ ions and the five negative charges due to three phenolates (L_a-3 H) and the two methoxy ligands (from the exchange of ligand during ESI-MS using CH₃OH as flowing phase) result in a single positively charged species. A similar analysis can also be applied to Fe₂L_b.

pBR322 DNA Cleavage by Binuclear Fe^{III} Complexes

In the absence of any added reductant or oxidant, when plasmid DNA pBR322 (0.02 μg μL⁻¹, 32 μm bp) is incubated at 37 °C for 1 h in 20 mM HEPES at pH 7.0 with Fe₂L_a or Fe₂L_b, activity can already be observed with less than 50 μM of the catalysts and DNA becomes converted from supercoiled (form I) to nicked (form II) to an extent which depends on the concentration of the dinuclear complexes (Figure 1). A comparison between the activity of Fe₂L_a and Fe₂L_b provided clear evidence for the important role of the acridine subunit in promoting the efficiency of cleavage, while just 5 μM Fe₂L_b is required to cleave 81% of supercoiled DNA after 1 h at 37 °C, the concentration of Fe₂L_a necessary to provide the same effect is more than 20 μM. From Figures 2 and 3 it may also be seen that the relative amount of supercoiled plasmid DNA decreases upon increasing the incubation time. Through exponential decay fitting, the rate constant of the supercoiled DNA

cleavage for $20\ \mu\text{M}$ Fe_2L_b was determined to be $1.0 \times 10^{-2}\ \text{s}^{-1}$ (Figure S12) which corresponds to a half-life of a minute. The rate constant represents a 14-fold increase in the cleavage efficiency when compared with the Fe_2L_a species ($7.1 \times 10^{-4}\ \text{s}^{-1}$, Figure S13). A similar rate acceleration (15-fold) was also reported by Tecilla et al. with a Zn-triaminocyclohexane complex tethered to an anthraquinone intercalator.^[28] In order to verify the impact of the intercalation, we carried out the cleavage experiments in the presence of the mixture of acridine ($5\ \mu\text{M}$) and Fe_2L_a ($5\ \mu\text{M}$). As shown in Figure S14, the extent of DNA cleavage by the mixture of acridine and Fe_2L_a is similar to Fe_2L_a and the activity is much less than for Fe_2L_b (covalently linked with acridine). Furthermore, the kinetic experiment using the mixture show cleavage rate for form I is $6.9 \times 10^{-4}\ \text{s}^{-1}$ (Figure S15–S16) which is also similar to Fe_2L_a ($7.1 \times 10^{-4}\ \text{s}^{-1}$). In contrast, the rate constant of Fe_2L_b is much larger ($1.0 \times 10^{-2}\ \text{s}^{-1}$). All of this evidence indicates that conjugation between the acridinium group and the diiron(III) subunit is necessary to get a fast cleavage rate.

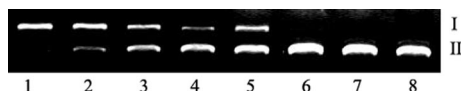


Figure 1. Agarose gel electrophoresis of pBR322 plasmid DNA treated with Fe_2L_a (lane 2–4) and Fe_2L_b (lane 5–8) for 1 h in an HEPES buffer (20 mM, pH 7.0) at 37°C . Lane 1: control DNA, lane 2: Fe_2L_a 10 μM , lane 3: Fe_2L_a 20 μM , lane 4: Fe_2L_a 50 μM , lane 5: Fe_2L_b 5 μM , lane 6: Fe_2L_b 10 μM , lane 7: Fe_2L_b 20 μM , lane 8: Fe_2L_b 50 μM .

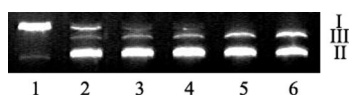


Figure 2. Time-dependence of pBR322 plasmid DNA cleavage by $20\ \mu\text{M}$ Fe_2L_a in an HEPES buffer (20 mM, pH 7.0) at 37°C . Lane 1: control, lane 2: Fe_2L_a 30 min, lane 3: 1 h, lane 4: 2 h, lane 5: 4 h, lane 6: 16 h.

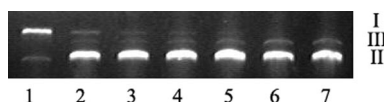


Figure 3. Time-dependence of pBR322 plasmid DNA cleavage by $20\ \mu\text{M}$ Fe_2L_b in an HEPES buffer (20 mM, pH 7.0) at 37°C . Lane 1: control, lane 2: Fe_2L_b 5 min, lane 3: 10 min, lane 4: 15 min, lane 5: 20 min, lane 6: 30 min, lane 7: 50 min.

The DNA cleaving systems based on mono-ferric complexes mostly involve the Fe^{II} ion and DNA cleavage by these systems, such as Fe-bleomycin and the Fenton agent, occur by an oxidative mechanism. The Fe^{III} -based agents so far reported are relatively few although Fe^{III} is present in the active site of some phosphatases. Two Fe^{III} complexes with high hydrolytic activity in DNA cleavage have been reported and both of them are binuclear. The first complex $\text{Fe}_2(\text{HPTB})$, described by Schnaith, Que and co-workers in 1994^[25] showed a surprising reactivity: in the presence of the complex at a concentration of $10\ \mu\text{M}$ at 25°C and a

pH of 8.0, the supercoiled form was completely degraded immediately after mixing. However, the cleavage system was very complicated because high activity depended on “oxidative” conditions, i.e. the presence of H_2O_2 or O_2 and a reductant (dithiothreitol or ascorbate). No rate constant was reported which might result from the fact that the cleavage occurred with the initial burst of activity and the extent of cleavage did not increase after lengthening the reaction time. The second diiron(III) complex $\text{Fe}_2(\text{DTPB})$ was investigated by Liu and co-workers.^[23] In the presence of such a complex at 37°C , a pH of 7.0 and a concentration of $100\ \mu\text{M}$, the supercoiled DNA was degraded with a rate constant of $2.0 \times 10^{-3}\ \text{s}^{-1}$ and the cleavage did not depend on the presence of O_2 . Compared with $\text{Fe}_2(\text{DTPB})$, the activity of Fe_2L_a seems somewhat lower ($7.1 \times 10^{-4}\ \text{s}^{-1}$) at $20\ \mu\text{M}$. However, for Fe_2L_b with a rate constant of $1.0 \times 10^{-2}\ \text{s}^{-1}$ at a concentration as low as $20\ \mu\text{M}$, the cleavage efficiency is evidently better than for $\text{Fe}_2(\text{DTPB})$.

Complex–DNA Interaction

The DNA binding ability of Fe_2L_b was studied using UV spectroscopy by following the absorbance intensity changes of the acridine group at 253 nm. Upon addition of increasing amounts of DNA to the complex, 48% hypochromism was observed (Figure 4) which indicates the interaction between acridine group and DNA. From the plot of $[\text{DNA}]/(\epsilon_a - \epsilon_f)$ vs. $[\text{DNA}]$, the intrinsic binding constant of the complex with DNA was calculated to be $(5.0 \pm 0.1) \times 10^5\ \text{M}^{-1}$. The moderate binding for this complex is comparable to those observed for many other acridine derivatives.^[33]

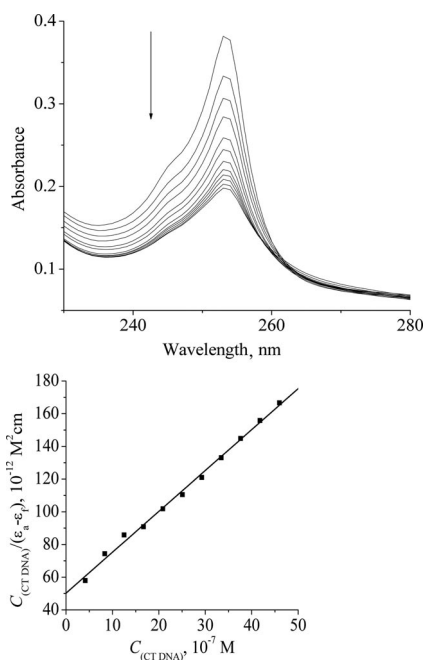


Figure 4. Top: absorption spectra of Fe_2L_b ($0.67 \times 10^{-5}\ \text{M}$) in the presence of increasing amounts of CT DNA ($6.27 \times 10^{-4}\ \text{M}$) at 25°C . Bottom: plot of $[\text{DNA}]/(\epsilon_a - \epsilon_f)$ vs. $[\text{DNA}]$.

As a means for further clarifying the binding of the binuclear complex, viscosity measurements were carried out on calf thymus DNA by varying the concentration of the complex. Acridine, a classical intercalator, causes a moderated increase in the viscosity of the DNA solution due to the separation of base pairs at intercalation sites and hence an increase in overall DNA length (Figure 5). In contrast, Fe_2L_a causes a decrease in DNA solution viscosity under the same conditions which can be attributed to the binding between Fe_2L_a and DNA through charge affinity leading to a distortion of the DNA structure. Compared with Fe_2L_a , Fe_2L_b further decreases the viscosity of DNA and the result suggests that the cooperation between the diiron complex and the acridine subunit makes distortion of the DNA more intense. The thermal denaturation studies show that the addition of Fe_2L_b to the calf thymus DNA could raise T_m from $(78.3 \pm 0.2)^\circ\text{C}$ to $(80.0 \pm 0.5)^\circ\text{C}$ but no change was observed in the case of Fe_2L_a (Figure S17). The CD spectra also show the difference in the interaction between Fe_2L_a and Fe_2L_b with CT DNA (Figure S18): Incubation of DNA and Fe_2L_a caused the intensities of both the positive and negative ellipticity bands to decrease, while incubation of DNA and Fe_2L_b caused the intensities of the negative ellipticity band to increase and the positive ellipticity band blue-shift. This suggests the acridine moiety has a significant effect on the conformational changes of DNA.

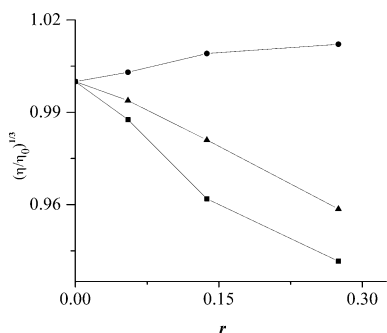


Figure 5. Effect of increasing the amounts of the compounds on the relative specific viscosity of calf thymus DNA. Viscosity is presented as $[\eta/\eta_0]^{1/3}$ in accord with the theory of Cohen and Eisenberg (1969). ● acridine + CT DNA, ▲ Fe_2L_a + CT DNA, ■ Fe_2L_b + CT DNA. $r = C_{\text{compound}}/C_{\text{DNA}}$.

Cleavage Mechanism Analysis

The earlier two diiron(III) complexes $\text{Fe}_2(\text{DTPB})$ and $\text{Fe}_2(\text{HPTB})$, described respectively by Liu^[23] and by Que,^[25] have shown the yielding linearised DNA can be quantitatively relegated by confirming the occurrence of a hydrolytic mechanism. In our cases, the linearised DNA has also been relegated by T4 ligase (Figure 6), although the relegation is not complete. In some cases, the hydrolytic products either did not end at the required 5'-phosphate and 3'-OH (ribose) termini or the complex sometimes bound to the termini of cleaved DNA. These reasons would result in the relegation being incomplete or even failing completely.^[34,35] To explore the effects of molecular oxygen on the degrada-

tion of DNA by the complexes, reactions were also performed under anaerobic conditions (Figure S19) and the results showed that Fe_2L_a and Fe_2L_b still effectively cleaved pBR322 DNA with little inhibition. In contrast, the oxidative cleaving system $\text{Fe}(\text{EDTA})^{2-}/\text{DTT}$ showed very strong oxygen dependence. Another general way to discriminate the hydrolytic mechanism from the oxidative mechanism is the examination of the DNA cleavage in the presence of reactive oxygen species (ROS) scavengers. Figure 7 indicates little effect on the cleavage efficiency of DNA with Fe_2L_b when DMSO or NaN_3 are added and superoxide dismutase (SOD) can even promote the cleavage efficiency. The experimental results suggest that hydroxyl radical, singlet oxygen and superoxide are not involved in the diiron DNA cleavage system. Additionally, the possibility of hydroxyl radical formation in the presence of Fe_2L_a can also be evaluated by monitoring the changes in absorbance at 552 nm for the dye rhodamine B. Degradation of the dye can provide a direct measure of the concentration of the hydroxyl radical formed.^[36] In the presence of Fe_2L_a , no obvious decrease in absorbance of the dye was detected over the time of the experiment (Figure S20) even after H_2O_2 was added, indicating that the hydroxyl radical is not formed under these conditions. An oxidative pathway can therefore be ruled out in the cleavage of DNA by diiron(III) complexes and, evidently, the cleavage occurs through a hydrolytic mechanism.

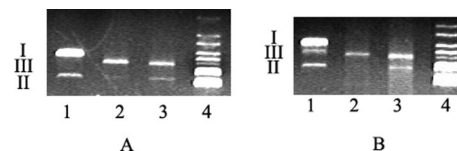


Figure 6. Ligation of pBR322 DNA cleaved by Fe_2L_a and Fe_2L_b . A, lane 1: supercoiled (upper) and nicked (lower) pBR322 DNA, lane 2: linearised pBR322 DNA cleaved by Fe_2L_a , lane 3: ligation of linearised pBR322 DNA by T4 DNA ligase, lane 4: λ DNA-EcoT14 I digest markers. B, lane 1: supercoiled (upper) and nicked (lower) pBR322 DNA, lane 2: linearised pBR322 DNA cleaved by Fe_2L_b , lane 3: ligation of linearised pBR322 DNA by T4 DNA ligase, lane 4: λ DNA-EcoT14 I digest markers.

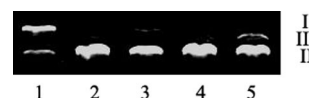


Figure 7. Agarose gel electrophoresis of pBR322 plasmid DNA treated with complex Fe_2L_b in various inhibitors of ROS. Incubation time: 1 h (37°C). Lane 1: control, lane 2: Fe_2L_b , 50 μM , lane 3: Fe_2L_b , 50 μM + 1 mM DMSO, lane 4: Fe_2L_b , 50 μM + 1 mM NaN_3 , lane 5: Fe_2L_b , 50 μM + 10 U of SOD.

Hydrolysis of BNPP Catalysed by Fe_2L_a

Cleavage experiments of phosphodiesteres were also carried out to further verify the hydrolytic activity of diiron complexes. In these kinds of experiments, BNPP is often used as a DNA model compound in the assessment of phosphodiesterase activity. For ensuring the solubility of the binary of the catalyst-substrate compound, the mixed solu-

tion including DMSO (10 vol.-%) was used. The reaction was monitored by following the increase in the absorbance at 400 nm which indicates the release of NP from BNPP. The determination of the initial rates at a pH of 7.36 as a function of substrate concentration revealed saturation kinetics with Michaelis–Menten-like behaviour (Figure 8). A linearisation after Lineweaver–Burke gave the following kinetics values: $K_M = (3.1 \pm 0.1) \times 10^{-3}$ M, $V_{\max} = (3.1 \pm 0.6) \times 10^{-9}$ mol L⁻¹ s⁻¹, and the catalytic constant $k_{\text{cat}} = V_{\max}/[\text{Fe}_2\text{L}_a]_0 = (5.2 \pm 0.2) \times 10^{-5}$ s⁻¹. The second-order rate constant, $k_{\text{BNPP}} (= k_{\text{cat}}/K_M)$ for BNPP is $(1.7 \pm 0.1) \times 10^{-2}$ M⁻¹ s⁻¹ and the substrate binding constant $K_b = 1/K_M = (3.2 \pm 0.1) \times 10^2$ M⁻¹. From the kinetic data obtained under these conditions, a rate acceleration toward BNPP of ca. $(4.7 \pm 0.2) \times 10^6$ times was found. The rate is comparable to that observed for other binuclear transition metal-based complexes.^[17]

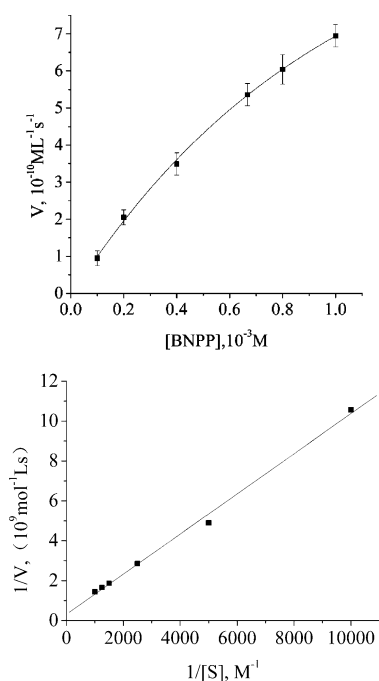


Figure 8. Top: saturation kinetic experiments for the cleavage of BNPP by Fe_2L_a at a pH of 7.36 and 50 °C. $I = 0.10$ M (NaNO_3), $[\text{Fe}_2\text{L}_a]_0 = 0.06$ mM, $[\text{HEPES buffer}] = 50$ mM, 10 vol.-% DMSO solution. Bottom: Lineweaver–Burke plot.

It was noted that the pH dependence of the catalytic activity between pH values of 5.9 and 8.5 shows a bell-shaped profile (Figure 9) with an optimum point at about pH 7.0. On the other hand, potentiometric titration of Fe_2L_a shows two successive titratable protons in a 1:9 DMSO/ H_2O solvent mixture (Figure 10). Sigmoidal fitting gives the $\text{p}K_a$ values of 5.3 and 8.5, respectively. From the titration curve, we propose a processes according to the equilibria represented by Equations (1) and (2).

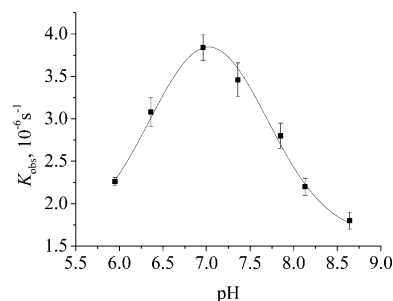
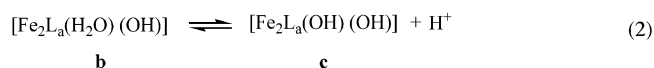
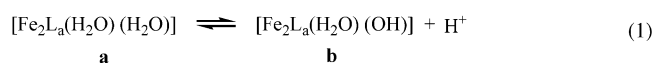


Figure 9. Dependence of the reaction rate on the pH under the following conditions: 10 vol.-% DMSO solution, 50 °C, $[\text{Fe}_2\text{L}_a] = 6.0 \times 10^{-5}$ mol L⁻¹, $[\text{BNPP}] = 2 \times 10^{-4}$ mol L⁻¹, $[\text{buffer}] = 5.0 \times 10^{-2}$ mol L⁻¹ (buffer: MES or HEPES), $I = 0.1$ mol L⁻¹ (NaNO_3).

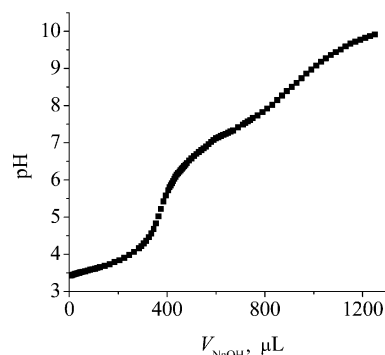


Figure 10. Potentiometric titration of Fe_2L_a (2.0×10^{-4} M) with an increasing amount of 0.01 M NaOH in DMSO/ H_2O (1:9).

The distribution curves (Figure 11) of the deprotonated products of Fe_2L_a in a 1:9 DMSO/ H_2O mixture display maximum monohydroxo species concentrations at a pH of 6.9 which is in good agreement with the optimum point for the catalytic activity at a pH of 7.0. These results indicate that the b species is the active species for the cleavage of phosphodiester. As proposed previously [equilibria (1) and (2)], monohydroxo species can provide a labile Fe–OH₂ bond for phosphodiester binding and another Fe^{III} bound hydroxide group for nucleophilic attack on the phosphorus atom. The decrease in the reactivity at pH > 7.0 most probably arises from the presence of the fully deprotonated form c, in which the tendency of the OH⁻ ion from the Fe–OH group to leave becomes reduced even though a more concentrated OH⁻ solution can increase the nucleophilic reactivity.

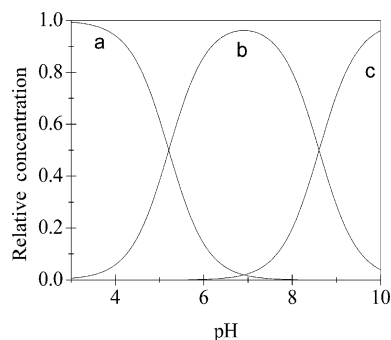


Figure 11. The distribution curves of the protonated products of Fe_2L_a in $\text{DMSO}/\text{H}_2\text{O}$ (1:9). (a): the binuclear Fe^{III} complex with two water molecules bound to the metal centre; b: the mono-hydroxo species and c: the dihydroxo one.

Conclusions

In summary, we have designed and synthesised a new diiron complex Fe_2L_b with an acridine group as an intercalator of DNA. The cleavage experiments indicate that the intercalative function can lead to a 14-fold increase in the cleavage efficiency. Furthermore, the hydrolytic mechanism studies demonstrate the potential of binuclear ferric complexes as catalyst models for artificial nucleases. In future work, we plan to link diiron(III) complexes with recognisable functional groups in the hope of realising the sequence-selective cleavage of DNA.

Experimental Section

General: When necessary, reactions and manipulations were carried out under an atmosphere of nitrogen. All reagents and solvents were analytical reagent grade and were used without further purification unless otherwise noted. UV/Vis spectra were recorded with a Lambda 35 UV/Vis spectrometer. ESI-MS spectra and high-resolution mass spectra were recorded on an HP 1100 MSD and an HPLC-Q-ToF MS (Micro) instrument, respectively. NMR spectra were recorded with a 400-MHz Varian INOVA system. IR spectra were obtained by using an FTIR-430 spectrometer. Elemental analyses were performed on a Vario EL III instrument. The potentiometric titration was performed on a PHS-3C pH meter. Viscosity measurements were recorded with a NXE-1B viscometer. Circular dichroism spectra of DNA were obtained with a JASCO J-20 automatic recording spectropolarimeter. The ImageMaster VDS system (Pharmacia Biotech) was used for electrophoresis experiments.

Syntheses

Bis(4-nitrophenyl) phosphates (BNPP) were prepared and purified following a modified literature method.^[37]

2-(4-Hydroxy-3,5-bis[(2-hydroxybenzyl)pyridin-2-ylmethylamino]methyl)benzyl)isoindole-1,3-dione (2) (Scheme S1): A solution of 2-[3,5-bis(chloromethyl)-4-hydroxybenzyl]isoindole-1,3-dione (0.61 g, 3.0 mmol), 2-[(pyridin-2-yl)methylamino]methyl]phenol (1.40 g, 6.5 mmol) and Et_3N in CH_2Cl_2 was stirred at ambient temperature for 2 d. The reaction mixture was then diluted with CH_2Cl_2 and washed with brine. The organic phase was dried with Na_2SO_4 and the solvent was removed by evaporation. Purification on silica gel using EtOAc as eluent gave the desired product (71%). ^1H NMR

(CDCl_3): δ = 8.60 (d, J = 4.4 Hz, 2 H, Py-H), 7.84 (m, 2 H, Py-H), 7.65–7.70 (m, 4 H, $\text{PhCH}_2\text{Ph-H}$), 7.26 (d, J = 6 Hz, 4 H, Py-H), 7.23 (t, J = 4.4 Hz, 2 H, Py-H), 7.10 (t, J = 7.2 Hz, 2 H, H-Ph), 7.02 (d, J = 7.2 Hz, 2 H, Ph-H), 6.72–6.76 (t, J = 7.2 Hz, 4 H, Ph-H), 4.71 (s, 2 H, $\text{Ph-CH}_2\text{-Ph}$), 3.83 (s, 4 H, $\text{N-CH}_2\text{-Py}$), 3.80 (s, 4 H, $\text{N-CH}_2\text{-Ph}$), 3.77 (s, 4 H, $\text{N-CH}_2\text{-Ph}$) ppm. ESI-MS: m/z 706.3 $[\text{M} + \text{H}]^+$, HRMS calcd. for $\text{C}_{43}\text{H}_{39}\text{N}_5\text{O}_5$ 706.3029, found 706.3022.

4-Aminomethyl-2,6-bis[(2-hydroxybenzyl)pyridin-2-ylmethylamino]methyl]phenol (3): Compound 2 (0.52 g, 7.4 mmol) was suspended in EtOH (10 mL) and hydrazine hydrate (0.22 g, 4.5 mmol) was added. The solution was heated to reflux for 2 h and stirred at ambient temperature overnight and the solvent was then evaporated under reduced pressure. The resultant solid was treated with 2 M HCl then extracted with CH_2Cl_2 and dried with Na_2SO_4 . Evaporation of the solvent yielded 0.36 g (85%) of the product. ^1H NMR (CD_3COCD_3): δ = 8.61–8.64 (m, 2 H, Py-H), 7.79 (dt, J = 7.7, 1.8 Hz, 2 H, Py-H), 7.32–7.38 (m, 4 H, Py-H), 7.07–7.14 (m, 6 H, Ph-H), 6.71–6.76 (m, 4 H, Ph-H), 4.30 (s, 2 H, $\text{Ph-CH}_2\text{-N}$), 3.87 (s, 4 H, $\text{N-CH}_2\text{-Py}$), 3.80 (s, 4 H, $\text{N-CH}_2\text{-Ph}$), 3.77 (s, 4 H, $\text{N-CH}_2\text{-Ph}$) ppm. ESI-MS: m/z 576.3 $[\text{M} + \text{H}]^+$. HR-MS calcd. for $\text{C}_{35}\text{H}_{37}\text{N}_5\text{O}_3$ 576.2975, found 576.2980.

5-(Acridin-9-yl)pentanoic Acid (4):^[31] Diphenylamine (1.69 g, 0.01 mol), hexanedioic acid (4.38 g, 0.03 mol) and anhydrous ZnCl_2 (6.8 g, 0.05 mol) were mixed well and heated at 230 °C for 20 h. H_2SO_4 (20 mL, 20 vol.-%) was then added to the reaction mixture which was subsequently heated to reflux for 4 h. The mixture was cooled and neutralised using aqueous NH_3 (25 vol.-%) solution. A solid product precipitated. After purification by silica gel column chromatography [eluted by a mixture (1:1) of EtOAc and petroleum ether], the pure compound was obtained. ^1H NMR (CD_3COCD_3): δ = 8.40 (d, J = 8.8 Hz, 2 H, Acr-H), 8.15 (d, J = 8.8 Hz, 2 H, Acr-H), 7.84 (t, J = 7.6 Hz, 2 H, Acr-H), 7.64 (t, J = 7.4 Hz, 2 H, Acr-H), 3.68 (t, J = 7.2 Hz, 2 H, CH_2Acr), 2.3 (t, J = 6.4 Hz, 2 H, CH_2COOH), 1.75 [m, 4 H, $-(\text{CH}_2)_2-$] ppm. ESI-MS m/z : 278.0 $[\text{M} - \text{H}]^-$.

5-(Acridin-9-yl)-N-(3,5-bis[(2-hydroxybenzyl)(pyridin-2-yl)methylamino]methyl)-4-hydroxybenzyl)pentanamide (L_b): 5-(Acridin-9-yl)pentanoic acid (0.126 g, 0.45 mmol) was heated to reflux in SOCl_2 (1 mL) for 2 h and the excess SOCl_2 was removed under reduced pressure. The dry solid was redissolved in dry acetonitrile (2 mL) and cooled in an ice bath. Compound 3 (0.22 g, 0.38 mmol) and triethylamine (0.5 mL) were added to the acetonitrile solution which was stirred under argon overnight as the temperature gradually returned to room temperature. Removing the solvent and purification on a column of silica gel using $\text{MeCN}/\text{H}_2\text{O}$ (95:5) as the eluent gave 0.16 g (50%) of the desired product. ^1H NMR (CD_3Cl): δ = 8.56 (d, J = 4.8 Hz, 2 H, Py-H), 8.35 (d, J = 8.8 Hz, 2 H, Acr-H), 8.2 (d, J = 8.8 Hz, 2 H, Acr-H), 7.77 (t, J = 7.6 Hz, 2 H, Acr-H), 7.60 (t, J = 7.8 Hz, 2 H, Py-H), 7.53 (t, J = 7.6 Hz, 2 H, Acr-H), 7.15–7.21 (m, 4 H, Py-H), 7.10 (t, J = 7.6 Hz, 2 H, Ph-H), 6.96 (s, 2 H, Ph-H), 6.92 (d, J = 8 Hz, 2 H, Ph-H), 6.79 (d, J = 6.4 Hz, 2 H, Ph-H), 6.93 (t, J = 7.6 Hz, 2 H, Ph-H), 6.36 (br., 1 H, $-\text{NHCO}-$), 4.27 (d, J = 5.2 Hz, 2 H, $\text{NH-CH}_2\text{-Ph}$), 3.77 (s, 4 H, $\text{N-CH}_2\text{-Py}$), 3.71 (s, 4 H, $\text{N-CH}_2\text{-Ph}$), 3.65 (s, 4 H, $\text{N-CH}_2\text{-Ph}$), 3.61 (t, J = 7.2 Hz, 2 H, $\text{CH}_2\text{-Acr}$), 2.34 (t, J = 7.2 Hz, 2 H, $\text{CH}_2\text{-CONH}$), 1.95–1.99 (m, 2 H, $-\text{CH}_2\text{CH}_2-$), 1.82–1.84 (m, 2 H, $-\text{CH}_2\text{CH}_2-$) ppm. ESI-MS m/z 837.5 $[\text{M} + \text{H}]^+$, HRMS calcd. for $\text{C}_{53}\text{H}_{52}\text{N}_6\text{O}_4$ 837.4128, found 837.4135.

Synthesis of the Binuclear Complexes $\text{Fe}_2\text{L}_a\text{Cl}_3 \cdot 3\text{H}_2\text{O}$ (Fe_2L_a) and $\text{Fe}_2\text{L}_b\text{Cl}_3 \cdot 4\text{H}_2\text{O}$ (Fe_2L_b): L_a (0.05 g, 0.09 mmol) and 2 equiv.

$\text{FeCl}_3 \cdot 6\text{H}_2\text{O}$ (0.049 g, 0.18 mmol) were dissolved in H_2O and heated at 50°C for 1 h to obtain a dark blue solution and the solution was then concentrated under reduced pressure. The target product Fe_2L_a was obtained as a solid residue. $\text{C}_{35}\text{H}_{39}\text{Cl}_3\text{Fe}_2\text{N}_4\text{O}_6$ ($\text{Fe}_2\text{L}_a\text{Cl}_3 \cdot 3\text{H}_2\text{O}$): calcd. C 50.66, H 4.74, N 6.75; found C 50.64, H 4.49, N 6.81. High-Resolution ESI-MS (CH_3OH as flowing phase) (Figure S1–S2) *m/z*: $[\text{Fe}^{\text{III}}\text{Fe}^{\text{III}}(\text{L}_{a-3\text{H}})(\text{OCH}_3)(\text{OCH}_3)]^+$ 731.1150; $[\text{Fe}^{\text{III}}\text{Fe}^{\text{III}}(\text{L}_{a-3\text{H}})(\text{OCH}_3)]^{2+}$, 350.1511. IR (KBr) (Figure S3): $\tilde{\nu} = 3427\text{--}3066$ (br., s), O–H of water and C–H of aromatic ring; 2922 (m) and 2855 (m), C–H of methane; 1609 (s) and 1475 (s), C=C of aromatic ring; 1264 (s), C–O of phenol; 759 cm^{-1} (s), C–H of aromatic ring. UV/Vis (H_2O): λ_{max} (ϵ_{m} , $\text{L mol}^{-1}\text{ cm}^{-1}$) (Figure S4): 260 (shoulder, 20000) attributed to the $\pi\text{--}\pi^*$ transition of the ligand; 531 nm (4400) attributed to the iron(III)–ligand charge transfer. Similarly, spectroscopic data of Fe_2L_b were obtained. $\text{C}_{53}\text{H}_{57}\text{Cl}_3\text{Fe}_2\text{N}_6\text{O}_8$ ($\text{Fe}_2\text{L}_b\text{Cl}_3 \cdot 4\text{H}_2\text{O}$): calcd. C 56.63, H 5.11, N 7.48; found C 56.92, H 4.45, N 7.62. High-Resolution ESI-MS (CH_3OH as flowing phase) (Figure S5–S9) *m/z*: $[\text{Fe}^{\text{III}}\text{Fe}^{\text{III}}(\text{L}_{b-3\text{H}})(\text{OCH}_3)\text{H}]^{3+}$ 325.6591; $[\text{Fe}^{\text{III}}\text{Fe}^{\text{III}}(\text{L}_{b-3\text{H}})(\text{OH})]^{2+}$ 480.9854; $[\text{Fe}^{\text{III}}\text{Fe}^{\text{III}}(\text{L}_{b-3\text{H}})(\text{OH})(\text{HCl})]^{2+}$ 498.9745; $[\text{Fe}^{\text{III}}\text{Fe}^{\text{III}}(\text{L}_{b-3\text{H}})(\text{OCH}_3)(\text{HCl})]^{2+}$ 505.9684; $[\text{Fe}^{\text{III}}\text{Fe}^{\text{III}}(\text{L}_{b-3\text{H}})(\text{OAc})(\text{HCl})]^{2+}$ 520.9583. IR (KBr) (Figure S10): $\tilde{\nu} = 3417\text{--}3000$ (br., s), O–H of water and C–H of aromatic ring; 2925 (m) and 2857 (m), C–H of methane; 1635 (s) and 1478 (s), C=C of aromatic ring; 1265 (strong), C–O of phenol; 759 cm^{-1} (strong), C–H of aromatic ring. UV/Vis (H_2O): λ_{max} (ϵ_{m} , $\text{L mol}^{-1}\text{ cm}^{-1}$) (Figure S11): 253 (56300) and 354 (13300) attributed to the $\pi\text{--}\pi^*$ transition of ligand; 531 nm (2980) attributed to the iron(III)–ligand charge transfer.

pBR322 DNA Cleavage Experiments by the Binuclear Metal Complexes: DNA cleavage experiments were performed using pBR 322 (Takara) in a 20 mM HEPES buffer, pH 7.0, with incubating DNA (0.4 μg) at 37°C in the presence and absence of the metal complex for the specified time. The cleavage reactions were stopped by addition of 3 μL of a loading buffer (0.25% bromphenol blue, 25% glycerol, 1 mM EDTA, 2% SDS). The electrophoresis of DNA cleavage products was performed on 1% agarose gel. The gels were run at 130 V for 45 min in a 0.01 M pH 7.0 TAE buffer. The resolved bands were visualised by ethidium bromide staining and were then quantified. A correction factor of 1.22 was utilised to account for the decreased ability of ethidium bromide to intercalate into form I DNA compared with forms II and III.^[38]

Cleavage of pBR322 in the Presence of ROS Scavengers: Scavengers of reactive oxygen intermediates (DMSO, NaN_3 and SOD) were added alternatively to the reaction mixtures. Cleavage was initiated by the addition of Fe_2L_b and stopped by 3 μL of a loading buffer (0.25% bromphenol blue, 25% glycerol, 1 mM EDTA, 2% SDS). Further analysis was conducted using the standard procedures described above.

Absorption Titration of Fe_2L_b Binding to DNA: The solutions of CT DNA gave a UV absorbance ratio at 260 and 280 nm, $A_{260}/A_{280} > 1.8$, indicating that the DNA was sufficiently free of protein.^[39] The concentrated stock solution of CT DNA (stored at 4°C and not used for more than 6 d) was prepared and the concentration of DNA in the nucleotide phosphate was determined by UV absorbance at 260 nm after a 1:10 dilution. The molar absorption coefficient of CT DNA was taken as $6600\text{ M}^{-1}\text{ cm}^{-1}$.^[39] A solution (3 mL) of $0.67 \times 10^{-5}\text{ M}$ Fe_2L_b in water was incubated for 30 min at 25°C . With addition of increasing amounts of 2 μL aliquots of DNA ($6.27 \times 10^{-4}\text{ M}$), the influence of volume was found to be negligible. The binding constant was determined using the following equation: $C_{\text{DNA}}/(e_a - e_f) = C_{\text{DNA}}/(e_b - e_f) + 1/K_b(e_b - e_f)$, where e_a , e_f , and e_b correspond to $A_{\text{obsd}}/[\text{complex}]$, the extinction coefficient

for the free iron complex and the extinction coefficient for the iron complex in the fully bound form, respectively. The intrinsic binding constant K_b was given by the ratio of the slope to intercept through the plot of $C_{\text{DNA}}/(e_a - e_f)$ vs. C_{DNA} .

Viscosity Measurements: Viscosity experiments were carried out on a NXE-1B viscometer at 25°C . The concentration of DNA was 280 μM in the nucleotide phosphate and the flow times were determined with a manually operated timer. Data were presented as $[\eta/\eta_0]^{1/3}$ vs. $[\text{complex}]/[\text{DNA}]$ (η is the viscosity of DNA solution in the presence of the compound and η_0 is the viscosity of DNA alone).

Ligation Experiment on the DNA Fragments: Enzymatic assays were performed using T4 DNA ligase to determine whether the cleaved products were consistent with hydrolysis of the phosphodiester linkages in DNA. First, the linearised DNA was isolated from the pBR 322 DNA cleavage products by Fe_2L_a or Fe_2L_b . Then, the following reaction was carried out for relegation: 1.5 μL of $10 \times$ ligation buffer, 10 μL of linearised pBR 322 DNA, 1 μL of T4 ligase (2 units), and 2.5 μL of H_2O were mixed and incubated at 16°C for 24 h. The ligation products were monitored by the electrophoresis and visualised by staining in an ethidium bromide solution.

Anaerobic Reactions: Deoxygenated water was prepared by four freeze-pump-thaw cycles. Before each cycle the water was equilibrated with nitrogen to assist the deoxygenating process. The deoxygenated water was stored under a nitrogen atmosphere prior to use. All anaerobic stock solutions were prepared in Schlenk tubes under nitrogen using the deoxygenated water. Reaction mixtures were prepared by the addition of the appropriate volumes of the stock solutions to the tubes and were incubated in a nitrogen-filled glovebag.

Thermal Denaturation of DNA: In 0.01 M Na_2HPO_4 buffer (pH 7.0), the absorption values of DNA as well the mixture of DNA and dinuclear Fe^{III} complexes at 260 nm were recorded by increasing the temperature in 5°C increments from 55°C to 95°C in a thermostatic bath where the controls were the buffer and the buffers in the absence and presence of the diiron complex, the concentration of which was the same as that in the sample.

CD Spectra Measurements: Circular dichroism spectra of DNA were obtained on a JASCO J-20 automatic recording spectropolarimeter operating at 25°C . The region between 200 and 300 nm was scanned for each sample.

Kinetic Measurements: The kinetic measurements were performed at 50°C in buffered solutions of a 1:9 mixture of DMSO/water. 2-(Morpholino)ethanesulfonic acid (MES) and 2-[4-(2-hydroxyethyl)piperazin-1-yl]ethanesulfonic acid (HEPES) were used as buffers. The ionic strength was fixed to 0.1 M with sodium nitrate. In a typical experiment, aqueous buffer solution (1.5 mL) was mixed with complex Fe_2L_a stock solution (in water) (0.9 mL) and DMSO (0.3 mL) in a temperature-controlled spectrometric cell. After the mixture was equilibrated for 15 min, BNPP stock solution (in water) was added (0.3 mL) and data collection was started immediately. The cleavage of BNPP was measured by following the increase in the absorption of 4-nitrophenolate (NP) at 400 nm. NP concentrations were determined using the molar extinction coefficients for NP of 2500, 4500, 9000, 12800, 16800, 17900, $19900\text{ M}^{-1}\text{ cm}^{-1}$ at pH values of 5.95, 6.36, 6.96, 7.36, 7.85, 8.13 and 8.64, respectively. The activities of the complexes were determined by the method of initial rates. At least three independent measurements were made.

Potentiometric Titration of Fe_2L_a : To an aqueous solution of Fe_2L_a ($2.0 \times 10^{-4}\text{ M}$) containing 10 vol.-% DMSO was added a solution of

0.01 M NaOH dropwise. Each data point was obtained by adding 2–20 μL of NaOH solution at 25 $^{\circ}\text{C}$.

Supporting Information (see also the footnote on the first page of this article): Synthesis of L_b (Scheme S1). High-Resolution ESI-MS spectrum of Fe_2L_a (Figure S1, S2). IR spectra of Fe_2L_a (Figure S3). Absorption spectra of 60 μM Fe_2L_a (Figure S4). High-Resolution ESI-MS spectrum of Fe_2L_b (Figure S5–S9). IR spectra of Fe_2L_b (Figure S10). Absorption spectra of 60 μM Fe_2L_b (Figure S11). Time course of DNA cleavage by 20 μM Fe_2L_b (Figure S12). Time course of DNA cleavage by 20 μM Fe_2L_a (Figure S13). Agarose gel electrophoresis of pBR322 DNA treated with Fe_2L_a , the mixture of acridine and Fe_2L_a , Fe_2L_b (Figure S14). Time-dependence of DNA cleavage by the mixture of 20 μM Fe_2L_a and 20 μM acridine (Figure S15). Time course of DNA cleavage by the mixture of 20 μM Fe_2L_a and 20 μM acridine (Figure S16). Thermal Denaturation studies of DNA (Figure S17). The CD spectra of CT DNA with complexes (Figure S18). Anaerobic and aerobic cleavage of pBR322 DNA by diiron(III) complexes and $\text{Fe}(\text{EDTA})^{2-}/\text{DTT}$ (Figure S19). Quantification of hydroxyl radicals by following the degradation of rhodamine B (Figure S20).

Acknowledgments

This work was supported by the Ministry of Education of China and National Natural Science Foundation of China (projects 20376010 and 20472012).

- [1] K. E. Erkkila, D. T. Odom, J. K. Barton, *Chem. Rev.* **1999**, *99*, 2777–2796.
- [2] K. Lang, J. Mosinger, D. M. Wagnerova, *Coord. Chem. Rev.* **2004**, *248*, 321–350.
- [3] H. T. Chifotides, K. R. Dunbar, *Acc. Chem. Res.* **2005**, *38*, 146–156.
- [4] A. Sreedhara, J. A. Cowan, *J. Biol. Inorg. Chem.* **2001**, *6*, 337–347.
- [5] W. K. Pogozelski, T. J. McNeese, T. D. Tuilius, *J. Am. Chem. Soc.* **1995**, *117*, 6428–6433.
- [6] C. J. Burrows, S. E. Rokita, *Acc. Chem. Res.* **1994**, *27*, 295–301.
- [7] M. D. Kuwabara, D. S. Sigman, *Biochemistry* **1987**, *26*, 7234–7238.
- [8] J. Stubbe, J. W. Kozarich, *Chem. Rev.* **1987**, *87*, 1107–1136.
- [9] J. Rammo, R. Hettich, A. Roigk, H. J. Schneider, *Chem. Commun.* **1996**, 105–107.
- [10] M. Yashiro, A. Ishikuno, M. Komiyama, *J. Chem. Soc., Chem. Commun.* **1995**, 1793–1794.
- [11] M. P. Fitzsimons, J. K. Barton, *J. Am. Chem. Soc.* **1997**, *119*, 3379–3380.
- [12] M. W. Göbel, *Angew. Chem. Int. Ed. Engl.* **1994**, *33*, 1141–1143.
- [13] F. H. Fry, A. J. Fischmann, M. J. Belousoff, L. Spiccia, J. Brugger, *Inorg. Chem.* **2005**, *44*, 941–950.
- [14] R. Ren, P. Yang, W. J. Zheng, Z. C. Hua, *Inorg. Chem.* **2000**, *39*, 5454–5463.
- [15] S. Matsuda, A. Ishikubo, A. Kuzuya, M. Yashiro, M. Komiyama, *Angew. Chem. Int. Ed.* **1998**, *37*, 3284–3286.
- [16] O. Iranzo, A. Y. Kovalevsky, J. R. Morrow, J. P. Richard, *J. Am. Chem. Soc.* **2003**, *125*, 1988–1993.
- [17] J. Chen, X. Y. Wang, Y. G. Zhu, J. Lin, X. L. Yang, Y. Z. Li, Y. Lu, Z. J. Guo, *Inorg. Chem.* **2005**, *44*, 3422–3430.
- [18] N. H. Williams, J. Chin, *Chem. Commun.* **1996**, 131–132.
- [19] N. H. Williams, W. Cheung, J. Chin, *J. Am. Chem. Soc.* **1998**, *120*, 8079–8087.
- [20] P. E. Jurek, A. M. Jurek, A. E. Martell, *Inorg. Chem.* **2000**, *39*, 1016–1020.
- [21] C. A. Chang, B. H. Wu, B. Y. Kuan, *Inorg. Chem.* **2005**, *44*, 6646–6654.
- [22] N. H. Williams, B. Takasaki, M. Wall, J. Chin, *Acc. Chem. Res.* **1999**, *32*, 485–493.
- [23] C. L. Liu, S. W. Yu, D. F. Li, Z. R. Liao, X. H. Sun, H. B. Xu, *Inorg. Chem.* **2002**, *41*, 913–922.
- [24] F. Verge, C. Lebrun, M. Fontecave, S. Menage, *Inorg. Chem.* **2003**, *42*, 499–507.
- [25] L. H. Schnaith, R. S. Hanson, L. Que Jr, *Proc. Natl. Acad. Sci. USA* **1994**, *91*, 569–573.
- [26] B. Vincent, G. L. Olivier-Lilley, B. A. Averill, *Chem. Rev.* **1990**, *90*, 1447–1467.
- [27] K. D. Copeland, M. P. Fitzsimons, R. P. Houser, J. K. Barton, *Biochemistry* **2002**, *41*, 343–356.
- [28] E. Bologgia, M. Gatos, L. Lucatello, F. Mancin, S. Moro, M. Palumbo, C. Sissi, P. Tecilla, U. Tonellato, G. Zagotto, *J. Am. Chem. Soc.* **2004**, *126*, 4543–4549.
- [29] G. Roelfes, M. E. Branum, L. Wang, L. Que Jr, B. L. Feringa, *J. Am. Chem. Soc.* **2000**, *122*, 11517–11518.
- [30] A. Neves, M. A. de Brito, I. Vencato, V. Drago, K. Griesar, W. Haase, *Inorg. Chem.* **1996**, *35*, 2360–2368.
- [31] V. E. Nadukkudy, S. Muthusami, R. Danaboyina, *Synth. Commun.* **1999**, *29*, 4007–4014.
- [32] F. Shi, H. Y. Li, X. J. Peng, R. Zhang, X. Q. Chen, J. L. Fan, L. C. Sun, *Chin. Chem. Lett.* **2004**, *15*, 1407–1410.
- [33] J. Joseph, E. Kuruvilla, A. T. Achuthan, D. Ramaiah, G. B. Schuster, *Bioconjugate Chem.* **2004**, *15*, 1230–1235.
- [34] M. Scarpellini, A. Neves, R. Hörner, A. J. Bortoluzzi, B. Szpoganics, C. Zucco, R. A. N. Silva, V. Drago, A. S. Mangrich, W. A. Ortiz, W. A. C. Passos, M. C. B. de Oliveira, H. Terenzi, *Inorg. Chem.* **2003**, *42*, 8353–8365.
- [35] C. Sissi, F. Mancin, M. Gatos, M. Palumbo, P. Tecilla, U. Tonellato, *Inorg. Chem.* **2005**, *44*, 2310–2317.
- [36] A. Sreedhara, J. D. Freed, J. A. Cowan, *J. Am. Chem. Soc.* **2000**, *122*, 8814–8824.
- [37] A. Williams, A. N. Richard, *J. Chem. Soc. B* **1971**, 1973–1979.
- [38] R. P. Hertzberg, P. B. Dervan, *J. Am. Chem. Soc.* **1982**, *104*, 313–315.
- [39] M. E. Reichmann, S. A. Rice, C. A. Thomas, P. Doty, *J. Am. Chem. Soc.* **1954**, *76*, 3047–3053.

Received: April 8, 2007

Published Online: October 16, 2007